Letter   Editors' Suggestion

Quantum logarithmic multifractality

Weitao Chen,[1,2,3] Olivier Giraud,[2,3,4] Jiangbin Gong,[1,2,3,*] and Gabriel Lemarié[2,3,5,†]

[1]*Department of Physics, National University of Singapore, Singapore 117543*
[2]*MajuLab, CNRS-UCA-SU-NUS-NTU International Joint Research Unit, Singapore*
[3]*Centre for Quantum Technologies, National University of Singapore, Singapore 117543*
[4]*Université Paris-Saclay, CNRS, LPTMS, 91405 Orsay, France*
[5]*Laboratoire de Physique Théorique, Université de Toulouse, CNRS, UPS, France*

(Received 29 December 2023; accepted 25 June 2024; published 31 July 2024)

Through a combination of rigorous analytical derivations and extensive numerical simulations, this work reports an exotic multifractal behavior, dubbed "logarithmic multifractality," in effectively infinite-dimensional systems undergoing the Anderson transition. In contrast to conventional multifractality observed in finite dimensions, logarithmic multifractality at infinite dimension introduces an algebraic behavior with respect to the logarithm of system size or time. We demonstrate this phenomenon across eigenstate statistics, spatial correlations, and wave packet dynamics. Our findings offer crucial insights into strong finite-size effects and slow dynamics in complex systems undergoing the Anderson transition, such as the many-body localization transition.

DOI: 10.1103/PhysRevResearch.6.L032024

Introduction. Determining the critical threshold of a continuous phase transition can be challenging. At finite system size, temperature, or time, such transition smoothens into a crossover, lacking singular behavior. While second-order phase transitions benefit from the scale-invariance property to discern their threshold [1], other transitions like Kosterlitz-Thouless (KT) type transitions [2] present additional complexities, including logarithmic finite-size effects [3].

A striking example of this fundamental difficulty is many-body localization (MBL), which prevents an isolated quantum many-body system from thermalizing under sufficiently strong disorder [4–7]. Despite mathematical arguments [8], and experimental [7] and numerical characterizations [6], the mere existence of this intriguing phase has been the subject of strong debate recently [9–22]. The primary reason for this debate is the lack of understanding of the critical behavior, including finite-size scaling and dynamical behavior at the transition.

Describing the critical behavior of such a transition, starting from a specific model, can be a daunting task, especially in the case of MBL, where we lack the powerful techniques available at low energies. However, two types of approaches have proven efficient in describing such universal properties: random graph and random matrix theories. MBL was initially conceived as an analogy to the problem of Anderson localization on random graphs [4,5,23]. In fact, the Anderson case provides analytical tools while retaining the subtle finite-size and finite-time effects typically observed in MBL [24–53].

Another powerful tool is random matrix theory [54]. In this context, it has enabled the description of properties across different phases, including the many-body thermal [55], the noninteracting metallic, and the Anderson localized phases, as well as the multifractal properties emerging at the Anderson transition in finite dimensions [56,57]. Recently, new random matrix ensembles have been developed to describe an extended nonergodic phase analogous to MBL [58–67].

In this Letter, along with the companion paper [68], we introduce and address analytically and numerically random matrix ensembles describing the critical properties at the Anderson transition in infinite dimensions (AT^{∞}). While this does not yet address the behavior at the MBL transition, it represents a significant step toward understanding it. Indeed, we are able to characterize analytically and numerically the logarithmically slow finite-size and finite-time effects that affect the AT^{∞}, similar to those observed in the context of MBL under strong disorder [19,46]. Our introduced random matrix models not only recover the critical behavior predicted for random regular and Erdös-Rényi graphs [26,27,43], but also predict another critical behavior termed "logarithmic multifractality." This behavior involves properties varying algebraically with the logarithm of system size or time.

Quantum multifractality: from finite to infinite dimensions. The Anderson transition is a well-studied second-order phase transition in finite dimensions [57,69]. Scale invariance at criticality manifests as quantum multifractality [37,70–87], a property depicting spatial fluctuations of eigenstates characterized by a set of fractal dimensions [88–90]. It can be investigated by considering the moments $P_q \equiv \sum_i |\psi(i)|^{2q}$ of

*Contact author: phygj@nus.edu.sg
†Contact author: lemarie@irsamc.ups-tlse.fr

order q of on-site eigenstate amplitudes $|\psi(i)|^2$ exhibiting an algebraic scaling behavior $P_q \sim N^{-D_q(q-1)}$ with the system size N. While $D_q = 1$ for ergodic delocalization and $D_q = 0$ for localization, the multifractal dimension D_q is a nontrivial function of q with $0 < D_q < 1$ at the transition point.

Various random matrix ensembles, such as the power-law random banded matrix (PRBM) [91–93] or the Ruijsenaars-Schneider (RS) [94–96] ensembles, which are generalizations of the Wigner-Dyson ensembles with power-law decaying off-diagonal elements, have been instrumental in describing analytically the critical multifractal behavior in finite dimensions [81,82,91–101]. Interestingly, they allow to describe how multifractal properties evolve from low dimensions $d \gtrsim 2$, where multifractality is weak, $D_2 \lesssim 1$, to high dimensions $d \gg 1$, where multifractality is strong, $D_2 \ll 1$.

One of the critical features of the infinite dimension case is its exotic multifractal properties, characterized by $D_q = 0$ for $q > q^*$, and $D_q > 0$ for $q < q^*$ [57], with a threshold $q^* = \frac{1}{2}$ [102–105]. However, the condition $D_q = 0$ for $q > q^*$ does not reliably identify the transition point, as knowledge of how D_q vanishes with system size is essential. For random regular and Erdős-Rényi graphs, it has been shown analytically that $P_2 \sim (\ln N)^{-1/2} + P_2^{\infty}$, where $P_2^{\infty} > 0$ signifies true localization behavior in the thermodynamic limit [26,27,43,52,53]. This type of critical behavior is termed "critical localization" in this Letter. By contrast, numerical simulations in hyperbolic and smallworld networks have suggested another possibility where P_2 is algebraic in $\ln N$, also compatible with $D_2 = 0$ [35,47,49,106]. This behavior hints at the possibility of log multifractality, i.e., $P_q \sim (\ln N)^{-d_q(q-1)}$, with a q-dependent log-multifractal exponent d_q.

Distinguishing between the above-mentioned two critical behaviors is crucial. Critical localization resembles a KT behavior in terms of P_2: Throughout the localized phase, P_2^{∞} remains finite until a sudden drop to zero in the delocalized phase, accompanied by characteristic logarithmic finite-size effects at the transition [43]. Markedly different, log multifractality entails the following scenario: localized wave functions on treelike graphs explore only a few rare branches [35,47,49]. This support spans $\ln N$ sites. At the transition, wavefunctions become multifractal on this support.

Based on both analytical and numerical simulations, the present work demonstrates the existence of log multifractality, in addition to the other critical localization behavior. We introduce a variant of the PRBM ensemble [91,92] emulating an effective infinite dimension by incorporating a specific decay of the off-diagonal matrix elements. We also introduce a unitary model akin to the so-called kicked rotor and RS models [95,96,107]. Also amenable to analytical treatment, the unitary model introduced here allows us to reach very large system sizes and times and therefore to validate the predicted log-multifractal properties. After characterizing log multifractality through the algebraic behavior of $P_q \sim (\ln N)^{-d_q(q-1)}$ in $\ln N$ both analytically and numerically, we explore the slow decay of eigenstate spatial correlations and derive characteristics of wave packet dynamics. As one remarkable consequence of log multifractality, we find that the return probability exhibits an algebraic decay with $\ln t$ rather than with the time variable t itself.

Random matrix models of infinite effective dimension. We aim to extend the PRBM ensemble to describe the critical behavior of the AT^{∞}. The PRBM consists of $N \times N$ real symmetric matrices $\hat{H}$, whose entries H_{ij} are independent Gaussian random variables with mean $\langle H_{ij}\rangle = 0$, variance $\langle |H_{ii}|^2\rangle = 1$, and $\langle |H_{ij}|^2\rangle \sim (b/|i-j|)^{-2a}$ for large $|i-j| \gg b$. The critical value $a = 1$ distinguishes between a delocalized phase ($a < 1$) and a localized phase ($a > 1$) [105]. While the PRBM model can be adjusted to emulate low to large but finite dimensions by controlling the bandwidth parameter b, infinite dimensionality, associated with $D_q \to 0$ as $N \to \infty$, appears to require $b = 0$. We address this obstacle by considering the limit $a \to 1^+$, i.e., the closest to localization while still being critical. Since $\lim_{\epsilon\to 0} |i-j|^{1+\epsilon} \simeq |i-j|(1 + \epsilon \ln|i-j|)$ for $\epsilon \ll 1$, we can retain the first-order term in $\ln|i-j|$ to obtain

$$\langle |H_{ij}|^2\rangle = \{1 + [|i-j| \ln^{1+\mu}(1 + |i-j|)/b]^2\}^{-1}, \qquad (1)$$

where we have generalized the logarithmic correction with an exponent $\mu \geqslant 0$. This defines the strongly multifractal random banded matrix (SRBM) ensemble. This ensemble enables us to analytically derive, when $\mu = 1/2 > 0$, key features of random regular graphs of infinite effective dimension [26,27,43,52,53], while also predicting the new log multifractality for $\mu = 0$, some features of which have been observed in smallworld and hyperbolic networks [35,47,49,106].

In addition to the above random Hermitian matrix ensemble, we also consider a unitary ensemble, named strongly multifractal random unitary matrix (SRUM) ensemble. The SRUM ensemble can be seen as a variant of the so-called kicked rotor model in quantum chaos and the RS model [95,96,107–109]. The SRUM ensemble is comprised of random unitary matrices

$$U_{ij} = e^{i\Phi_i} \sum_{k=1}^{N} F_{ik} e^{-iKV(2\pi k/N)} F_{kj}^{-1}, \qquad (2)$$

where $V(x) = \ln[-1/\ln(\lambda|\sin\frac{x}{2}|)]$ for $x \in [0, 2\pi)$, $V(x + 2\pi) = V(x)$ and the Fourier transform $F_{jk} = e^{2i\pi jk/N}/\sqrt{N}$. The parameter λ is set to $\lambda = 0.9$ to avoid the singularity of $V(x)$ at $x = \pi$. Φ_i are random phases uniformly distributed over $[0, 2\pi)$. Due to the singular behavior of $V(x)$ when $x \to 0$ (2π), the amplitudes of the matrix elements of U_{ij} decay as $|U_{ij}| \simeq K/(2r \ln r)$ for large $r \equiv |i-j|$; this is the same behavior as $\sqrt{\langle |H_{ij}|^2\rangle}$ in Eq. (1) with $\mu = 0$ and b replaced by $K/2$.

Log multifractality. To examine how log multifractality emerges when $\mu = 0$, we analytically compute $\langle P_q\rangle$ by treating the off-diagonal matrix elements in SRBM and SRUM models as perturbation [95,96]. The moments P_q for $q < \frac{1}{2}$ can be obtained through a standard perturbative approach [68] which yields, for the SRUM model at lowest order in K,

$$\langle P_q\rangle \simeq 1 + K^{2q} A_q (\ln N)^{-2q} N^{-D_q(q-1)}, \quad D_q = \frac{2q-1}{q-1}, \qquad (3)$$

with A_q a constant. For large N, we approach the conventional multifractal behavior $P_q \sim N^{-D_q(q-1)}$.

Importantly, this approach leads to divergences when $q > \frac{1}{2}$, necessitating more advanced treatments. In this context, we employ Levitov renormalization [97,98], known for

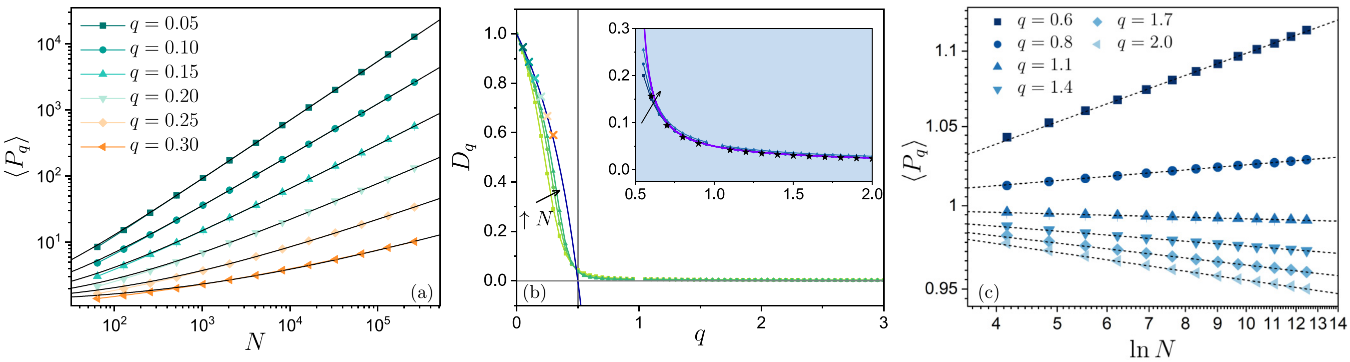

FIG. 1. Eigenstate log multifractality in the SRUM model. (a) Conventional multifractality for moments P_q with $q < \frac{1}{2}$ as predicted by Eq. (3) for $K = 0.05$ and different q values as indicated by the labels. The black dashed lines are fits by Eq. (3) with A_q and D_q two fitting parameters. (b) Multifractal dimension D_q vs q for $K = 0.05$. The finite-size estimate $D_q \equiv [\log_2\langle P_q(N/2)\rangle - \log_2\langle P_q(N)\rangle]/[q-1]$, represented by green symbols (lines are an eyeguide) for system sizes $N = 2^{10}, 2^{14}, 2^{18}$, converges slowly to the theoretical prediction $D_q = (2q-1)/(q-1)$ for $q < 1/2$. The crosses indicate the D_q values obtained from the fits from Eq. (3) represented in panel (a), which incorporate the log corrections and agree perfectly well with $D_q = (2q-1)/(q-1)$. Inset: Log-multifractal dimension d_q (computed as $[\ln\langle P_q(N/2)\rangle - \ln\langle P_q(N)\rangle]/[(q-1)(\ln\ln N - \ln\ln \frac{N}{2})]$) as a function of q for system sizes $N = 2^{10}, 2^{14}, 2^{18}$. d_q converges at large N to the nontrivial analytical law (4) (violet line). Star symbols are fitted d_q values shown in panel (c). (c) Log multifractality for moments with $q > \frac{1}{2}$, well described by Eq. (4). Different curves correspond to different q values as indicated by the labels. The black dashed lines are power-law fits $\langle P_q\rangle = c(\ln N)^{-d_q(q-1)}$ with c and d_q two fitting parameters, see inset of panel (b). Disorder averaging ranges from 360 000 realizations for $N = 2^6$ to 1800 realizations for $N = 2^{18}$. Error bars are smaller than symbol size.

its effectiveness in the PRBM and RS ensembles [92,95]. This yields (see [68] for details) the following expression for $q > \frac{1}{2}$ and $K \ll 1$:

$$\langle P_q\rangle \sim (\ln N)^{-d_q(q-1)}, \quad d_q = \frac{K\Gamma(q-\frac{1}{2})}{\sqrt{\pi}\,\Gamma(q-1)(q-1)}. \tag{4}$$

Similar treatments apply to SRBM and also give Eq. (3) and Eq. (4), with K replaced by $4b$ [68]. In this regard, results from SRUM and SRBM fully echo each other, illustrating their universality. Equation (4) shows that our models display log multifractality, as P_q algebraically scales with $\ln N$ rather than N, and provides an explicit expression for the corresponding multifractal exponent.

To validate the analytical predictions (3) and (4), especially the algebraic behavior in $\ln N$, reaching large system sizes is essential. This is much easier to achieve in the SRUM case. Indeed, implementing a sparse diagonalization approach assisted by a polynomial filter [110], we are able to explore system sizes as large as $N = 2^{18}$ with a high number of random realizations. In Fig. 1, the left panel illustrates the conventional multifractal behavior of moments P_q with $q < \frac{1}{2}$, fitting well with Eq. (3). The multifractal dimension D_q is displayed as a function of q in the middle panel, vanishing for $q > \frac{1}{2}$. The right panel showcases the log multifractality of moments P_q with $q > \frac{1}{2}$, fitting effectively with Eq. (4). The log-multifractal dimension d_q exhibits a nontrivial dependency on q and K, well accounted for by Eq. (4). These results are also verified for the SRBM case, see [68], thus supporting their universality.

We now turn to the average correlation function, $C(r) \equiv \langle\sum_{i=1}^{N}|\psi(i)|^2|\psi(i+r)|^2\rangle$, a key multifractality probe which illustrates particularly well the distinctive features of log multifractality induced by the effective infinite dimension of our models (see [68] for more details). We find that it exhibits an exotic behavior given by $C(r) \sim (1/r) \times (\ln r)^{-\alpha}$, with $0 < \alpha < 1$, as depicted in Fig. 2(b). The specific decay of $C(r)$ associated with log multifractality can be understood as the product of two terms. The first $1/r$ factor indicates the nontrivial logarithmic wavefunction support, reminiscent of the behavior found in random graphs of effective infinite dimension, where wavefunctions explore a finite number of branches, thus a logarithmic number of sites, from the exponentially large number of branches at disposal [29,35,47,49]. In fact, the $1/r$ prefactor replaces the K^{-r} term found in such correlation function in random graphs, see, e.g., Eq. (4) of [47]; it is therefore a hallmark of the effective infinite dimension of our models. The second term comes from the replacement of $C(r) \sim r^{D_2-1}$ obtained in conventional multifractality by a power function of $\ln r$ to reflect multifractality in $\ln N$ [Eq. (4)]. Hence, it is a signature of multifractality on a logarithmic support with distances scaling as $\ln r$ instead of r.

Wave packet dynamics. The dynamics of a wave packet initialized at a single site $\psi(r, t = 0) = \delta_{r,0}$ also encodes rich information on quantum multifractality [81,84,86,87,111]. In conventional multifractality, the return probability $R_0(t) \equiv |\langle\psi(t)|\psi(0)\rangle|^2$ exhibits a power-law decay with time t, $\langle R_0\rangle \sim t^{-D_2}$, with an exponent given by the multifractal dimension D_2 [80–82]. To describe analytically $R_0(t)$ in the case of log multifracality, we focus on the SRBM model and adapt the analytic expression for the return probability that was obtained for the PRBM case in the limit $b \ll 1$ by means of a supersymmetric virial expansion [82], see [68] for more details. This approach gives $\langle R_0\rangle \sim (\ln t)^{-d_2}$, which indicates an algebraic decay of $\langle R_0\rangle$ in $\ln t$ controlled by the log-multifractal dimension d_2.

On the other hand, for a finite size N, the limit $t \to \infty$ gives $\langle R_0\rangle \sim \langle P_2\rangle \sim (\ln N)^{-d_2}$ [see Eq. (4)]. Therefore, there must exist a characteristic time scale t^* separating the infinite-size behavior $\sim(\ln t)^{-d_2}$ of $\langle R_0\rangle$ from its finite-size stationary value $\sim(\ln N)^{-d_2}$, with $\ln t^* \sim \ln N$. We can hence assume, as

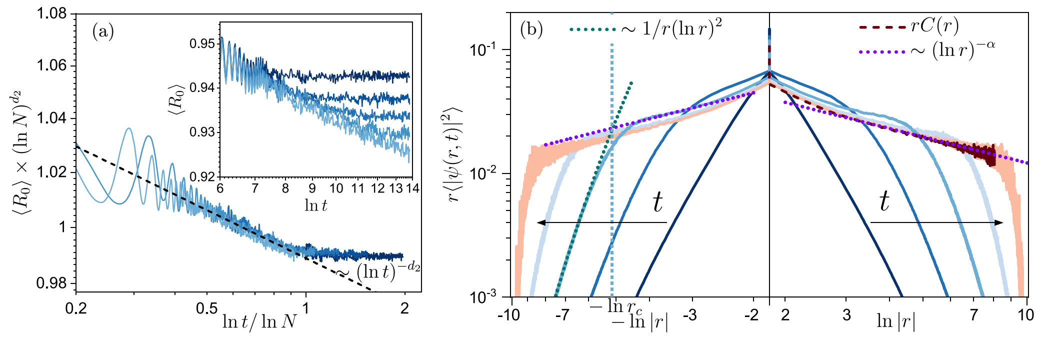

FIG. 2. Slow wave packet dynamics for the SRUM with initial state $\psi(r, t = 0) = \delta_{r,0}$, in connection with log multifractality. (a) Illustration of the scaling property in Eq. (5) for the return probability $\langle R_0 \rangle$ at $K = 0.05$. The data from various system sizes and times $t \in [10, 10^6]$ collapse onto a single scaling curve when $\langle R_0 \rangle \times (\ln N)^{d_2}$ is plotted against the scaled time $\ln t / \ln N$. The black dashed line represents a power-law fit, $\langle R_0 \rangle \sim (\ln t)^{-d_2}$, giving $d_2 \approx 0.025$ in perfect agreement with the analytical prediction $d_2 = K/2$ and the value extracted from P_2. Inset: corresponding raw data for $\langle R_0 \rangle$ with, from top to bottom, $N = 2^7, 2^9, \ldots, 2^{15}$. Results are averaged over a range from 18 000 realizations for $N = 2^7$ to 7200 realizations for $N = 2^{15}$. (b) Average probability distribution of the wave packet at different times plotted as $r\langle|\psi(r,t)|^2\rangle$ vs $\ln r$ in a symmetrical log-log scale, with $K = 1.0$. Curves from dark blue to pale orange correspond to evolution times $t = 10, 77, 1668, 35398, 10^5$. The violet dotted line fits the behavior expected at short distances $r \ll r_c$, corresponding to the correlation function $C(r)$ (shown by the maroon dashed line), giving $\alpha \approx 0.7$; while the green dotted line fits the one for $r \gg r_c$, see Eq. (6). The vertical dashed line locates the crossover r_c. Results are averaged over 720 000 [36 000 for $C(r)$] disorder configurations with system size $N = 2^{15}$ [$N = 2^{16}$ for $C(r)$].

was done in [87], the following scaling behavior:

$$\langle R_0(t, N) \rangle = (\ln N)^{-d_2} g(\ln t / \ln N), \tag{5}$$

with $g(x) \sim_{x \ll 1} x^{-d_2}$ and $g(x) \sim_{x \gg 1}$ cst. The same scaling behavior is expected for SRUM ensemble, as the amplitudes of its off-diagonal elements decay in the same way. The results, shown in Fig. 2(a) for SRUM, confirm the validity of the scaling described by Eq. (5).

It is also interesting to examine the spatial expansion of a wave packet [86,87,111–113]. For sufficiently small r, we find that the wave packet amplitudes exhibit a decay behavior similar to the average spatial correlation function of the eigenstates, $C(r)$. Instead, for sufficiently large r, the wave packet amplitudes decay following the direct long-range couplings described by the off-diagonal matrix elements, i.e., Eq. (1). If we introduce r_c as the crossover scale between the two regimes, these two behaviors can be summarized as

$$\langle|\psi(r,t)|^2\rangle = \begin{cases} \langle R_0 \rangle [r(\ln r)^\alpha]^{-1}, & 1 < r < r_c, \\ B\left[\frac{r}{r_c}\ln(\frac{r}{r_c})\right]^{-2}, & r_c < r \leqslant \frac{N}{2}, \end{cases} \tag{6}$$

with $\ln r_c \sim (\ln t)^{d_2/(1-\alpha)}$ and $B = \langle R_0 \rangle [r_c(\ln r_c)^\alpha]^{-1}$, see [68]. This behavior is illustrated in Fig. 2(b).

Generalization to critical localization. We can construct a whole family of SRBM ensembles describing critical localization if we consider $\mu > 0$ in Eq. (1). If we focus on the case of $q = 2$ only, analytical procedures as above lead to $\langle P_2 \rangle \sim (\ln N)^{-\mu} + P_2^\infty$, with $P_2^\infty > 0$ indicative of a localized behavior. Our results also reveal that the spatial correlation function of the eigenstates decays as $C(r) \sim 1/[r(\ln r)^{1+\mu}]$, and the return probability $R_0(t) \sim (\ln t)^{-\mu} + R_0^\infty$, with $R_0^\infty > 0$ (see [68] for more details). It is noteworthy that when $\mu = \frac{1}{2}$, these results align with the analytical predictions for random regular and Erdős-Rényi graphs [26,27,43]. This suggests a potential connection between the exponent μ and the specific characteristics of certain types of graphs.

Conclusion. In this Letter, we have presented two random matrix models for the critical behavior at the Anderson transition in infinite dimension. Through analytical solutions and extensive numerical simulations involving large size and time scales, we have provided compelling evidence of log multifractality, through the scaling behavior $\langle P_q \rangle \sim (\ln N)^{-d_q(q-1)}$ for $q > \frac{1}{2}$. This scaling behavior signifies a remarkable scale invariance in the logarithm of the system size, extending beyond conventional multifractality in finite dimension and scale invariance in second-order phase transitions. Logarithmic multifractality controls the slow decay of spatial correlations and the slow dynamics of a time-evolving wave packet, particularly its return probability $\langle R_0 \rangle \sim (\ln t)^{-d_2}$. Finally, we discussed how to generalize our random matrix models to obtain other "critical localization" scenarios predicted at the Anderson transition on random regular and Erdős-Rényi graphs [26,27,43].

This work thus uncovers distinctive characteristics of the Anderson transition in infinite dimensions. It would be interesting to investigate whether the critical behavior on smallworld or hyperbolic networks, where P_2 follows an algebraic law with $\ln N$ [35,47,49,106], suggesting log multifractality, conforms to our predictions. The multifractal delocalization on a logarithmic support that we find here is reminiscent of extended nonergodic wavefunctions with fractal support [58–67] and of the critical properties recently proposed for the Anderson transition in large dimension [114,115]. It would be interesting to characterize these critical behaviors along the lines drawn in our study.

Since the Anderson transition in infinite dimension is closely related to the elusive MBL transition, one perspective of this work is to formulate a random matrix model to describe the critical behavior at the MBL transition. While generalized RP random matrix models allow to describe transitions between ergodic, nonergodic, and localized phases [58–67], they lack the notion of spatial distance, which is crucial in such localization problems, and crucially rely on an explicit system size dependence of the matrix elements. In contrast, our models capture the universal physics of infinite dimensions through a specific and nontrivial spatial decay of hopping elements. Having an analytical description of the slow dynamics and strong finite-size effects expected at the MBL critical point will allow us to address the recent debate about the existence of MBL more effectively.

Acknowledgments. This study was supported by research funding Grants No. ANR-18-CE30-0017 and No. ANR-19-CE30-0013, and by the Singapore Ministry of Education Academic Research Fund Tier I (WBS No. R-144-000-437-114). We thank Calcul en Midi-Pyrénées (CALMIP) and the National Supercomputing Centre (NSCC) of Singapore for computational resources and assistance. W.C. is supported by the President's Graduate Fellowship at the National University of Singapore and the Merlion Ph.D. Scholarship awarded by the French Embassy in Singapore. J.G. acknowledges support by the National Research Foundation, Singapore and A*STAR under its CQT Bridging Grant.

[1] K. G. Wilson, The renormalization group and critical phenomena, Rev. Mod. Phys. **55**, 583 (1983).
[2] J. M. Kosterlitz, Kosterlitz–Thouless physics: a review of key issues, Rep. Prog. Phys. **79**, 026001 (2016).
[3] Y.-D. Hsieh, Y.-J. Kao, and A. W. Sandvik, Finite-size scaling method for the Berezinskii–Kosterlitz–Thouless transition, J. Stat. Mech.: Theory Exp. (2013) P09001.
[4] I. V. Gornyi, A. D. Mirlin, and D. G. Polyakov, Interacting electrons in disordered wires: Anderson localization and low-T transport, Phys. Rev. Lett. **95**, 206603 (2005).
[5] D. Basko, I. Aleiner, and B. Altshuler, Metal–insulator transition in a weakly interacting many-electron system with localized single-particle states, Ann. Phys. **321**, 1126 (2006).
[6] F. Alet and N. Laflorencie, Many-body localization: An introduction and selected topics, Comptes Rendus. Physique **19**, 498 (2018).
[7] D. A. Abanin, E. Altman, I. Bloch, and M. Serbyn, *Colloquium:* Many-body localization, thermalization, and entanglement, Rev. Mod. Phys. **91**, 021001 (2019).
[8] J. Z. Imbrie, On many-body localization for quantum spin chains, J. Stat. Phys. **163**, 998 (2016).
[9] W. De Roeck and F. Huveneers, Stability and instability towards delocalization in many-body localization systems, Phys. Rev. B **95**, 155129 (2017).
[10] A. Morningstar, L. Colmenarez, V. Khemani, D. J. Luitz, and D. A. Huse, Avalanches and many-body resonances in many-body localized systems, Phys. Rev. B **105**, 174205 (2022).
[11] D. Sels, Bath-induced delocalization in interacting disordered spin chains, Phys. Rev. B **106**, L020202 (2022).
[12] J. Léonard, S. Kim, M. Rispoli, A. Lukin, R. Schittko, J. Kwan, E. Demler, D. Sels, and M. Greiner, Signatures of bath-induced quantum avalanches in a many-body–localized system, Nat. Phys. **19**, 481 (2023).
[13] F. Weiner, F. Evers, and S. Bera, Slow dynamics and strong finite-size effects in many-body localization with random and quasiperiodic potentials, Phys. Rev. B **100**, 104204 (2019).
[14] J. Šuntajs, J. Bonča, T. Prosen, and L. Vidmar, Quantum chaos challenges many-body localization, Phys. Rev. E **102**, 062144 (2020).
[15] J. Šuntajs, J. Bonča, T. Prosen, and L. Vidmar, Ergodicity breaking transition in finite disordered spin chains, Phys. Rev. B **102**, 064207 (2020).
[16] M. Kiefer-Emmanouilidis, R. Unanyan, M. Fleischhauer, and J. Sirker, Slow delocalization of particles in many-body localized phases, Phys. Rev. B **103**, 024203 (2021).
[17] D. Sels and A. Polkovnikov, Dynamical obstruction to localization in a disordered spin chain, Phys. Rev. E **104**, 054105 (2021).
[18] L. Vidmar, B. Krajewski, J. Bonča, and M. Mierzejewski, Phenomenology of spectral functions in disordered spin chains at infinite temperature, Phys. Rev. Lett. **127**, 230603 (2021).
[19] D. Abanin, J. Bardarson, G. De Tomasi, S. Gopalakrishnan, V. Khemani, S. Parameswaran, F. Pollmann, A. Potter, M. Serbyn, and R. Vasseur, Distinguishing localization from chaos: Challenges in finite-size systems, Ann. Phys. **427**, 168415 (2021).
[20] P. Sierant, D. Delande, and J. Zakrzewski, Thouless time analysis of Anderson and many-body localization transitions, Phys. Rev. Lett. **124**, 186601 (2020).
[21] R. K. Panda, A. Scardicchio, M. Schulz, S. R. Taylor, and M. Žnidarič, Can we study the many-body localisation transition? Europhys. Lett. **128**, 67003 (2020).
[22] D. J. Luitz and Y. B. Lev, Absence of slow particle transport in the many-body localized phase, Phys. Rev. B **102**, 100202(R) (2020).
[23] B. L. Altshuler, Y. Gefen, A. Kamenev, and L. S. Levitov, Quasiparticle lifetime in a finite system: A nonperturbative approach, Phys. Rev. Lett. **78**, 2803 (1997).
[24] M. R. Zirnbauer, Localization transition on the Bethe lattice, Phys. Rev. B **34**, 6394 (1986).
[25] M. R. Zirnbauer, Anderson localization and non-linear sigma model with graded symmetry, Nucl. Phys. B **265**, 375 (1986).
[26] Y. V. Fyodorov and A. D. Mirlin, Localization in ensemble of sparse random matrices, Phys. Rev. Lett. **67**, 2049 (1991).
[27] A. D. Mirlin and Y. V. Fyodorov, Distribution of local densities of states, order parameter function, and critical behavior near the Anderson transition, Phys. Rev. Lett. **72**, 526 (1994).
[28] C. Monthus and T. Garel, Anderson localization on the Cayley tree: multifractal statistics of the transmission at criticality and off criticality, J. Phys. A: Math. Theor. **44**, 145001 (2011).
[29] G. Biroli, A. C. Ribeiro-Teixeira, and M. Tarzia, Difference between level statistics, ergodicity and localization transitions on the Bethe lattice, arXiv:1211.7334.
[30] A. De Luca, B. L. Altshuler, V. E. Kravtsov, and A. Scardicchio, Anderson localization on the Bethe lattice: Nonergodicity of extended states, Phys. Rev. Lett. **113**, 046806 (2014).
[31] B. L. Altshuler, E. Cuevas, L. B. Ioffe, and V. E. Kravtsov, Nonergodic phases in strongly disordered random regular graphs, Phys. Rev. Lett. **117**, 156601 (2016).
[32] K. S. Tikhonov, A. D. Mirlin, and M. A. Skvortsov, Anderson

localization and ergodicity on random regular graphs, Phys. Rev. B **94**, 220203(R) (2016).
[33] K. S. Tikhonov and A. D. Mirlin, Fractality of wave functions on a Cayley tree: Difference between tree and locally treelike graph without boundary, Phys. Rev. B **94**, 184203 (2016).
[34] M. Sonner, K. S. Tikhonov, and A. D. Mirlin, Multifractality of wave functions on a Cayley tree: From root to leaves, Phys. Rev. B **96**, 214204 (2017).
[35] I. García-Mata, O. Giraud, B. Georgeot, J. Martin, R. Dubertrand, and G. Lemarié, Scaling theory of the Anderson transition in random graphs: Ergodicity and universality, Phys. Rev. Lett. **118**, 166801 (2017).
[36] G. Biroli and M. Tarzia, Delocalized glassy dynamics and many-body localization, Phys. Rev. B **96**, 201114(R) (2017).
[37] E. Tarquini, G. Biroli, and M. Tarzia, Critical properties of the Anderson localization transition and the high-dimensional limit, Phys. Rev. B **95**, 094204 (2017).
[38] V. Kravtsov, B. Altshuler, and L. Ioffe, Non-ergodic delocalized phase in Anderson model on Bethe lattice and regular graph, Ann. Phys. **389**, 148 (2018).
[39] K. S. Tikhonov and A. D. Mirlin, Critical behavior at the localization transition on random regular graphs, Phys. Rev. B **99**, 214202 (2019).
[40] G. De Tomasi, S. Bera, A. Scardicchio, and I. M. Khaymovich, Subdiffusion in the Anderson model on the random regular graph, Phys. Rev. B **101**, 100201(R) (2020).
[41] G. Parisi, S. Pascazio, F. Pietracaprina, V. Ros, and A. Scardicchio, Anderson transition on the Bethe lattice: an approach with real energies, J. Phys. A: Math. Theor. **53**, 014003 (2020).
[42] S. Bera, G. De Tomasi, I. M. Khaymovich, and A. Scardicchio, Return probability for the Anderson model on the random regular graph, Phys. Rev. B **98**, 134205 (2018).
[43] K. S. Tikhonov and A. D. Mirlin, Statistics of eigenstates near the localization transition on random regular graphs, Phys. Rev. B **99**, 024202 (2019).
[44] S. Roy and D. E. Logan, Localization on certain graphs with strongly correlated disorder, Phys. Rev. Lett. **125**, 250402 (2020).
[45] G. Biroli, A. K. Hartmann, and M. Tarzia, Critical behavior of the Anderson model on the Bethe lattice via a large-deviation approach, Phys. Rev. B **105**, 094202 (2022).
[46] K. S. Tikhonov and A. D. Mirlin, From Anderson localization on random regular graphs to many-body localization, Ann. Phys. **435**, 168525 (2021).
[47] I. García-Mata, J. Martin, R. Dubertrand, O. Giraud, B. Georgeot, and G. Lemarié, Two critical localization lengths in the Anderson transition on random graphs, Phys. Rev. Res. **2**, 012020(R) (2020).
[48] L. Colmenarez, D. J. Luitz, I. M. Khaymovich, and G. De Tomasi, Subdiffusive Thouless time scaling in the Anderson model on random regular graphs, Phys. Rev. B **105**, 174207 (2022).
[49] I. García-Mata, J. Martin, O. Giraud, B. Georgeot, R. Dubertrand, and G. Lemarié, Critical properties of the Anderson transition on random graphs: Two-parameter scaling theory, Kosterlitz-Thouless type flow, and many-body localization, Phys. Rev. B **106**, 214202 (2022).
[50] C. Vanoni, B. L. Altshuler, V. E. Kravtsov, and A. Scardicchio, Renormalization group analysis of the Anderson model on random regular graphs, arXiv:2306.14965.
[51] M. Baroni, G. G. Lorenzana, T. Rizzo, and M. Tarzia, Corrections to the Bethe lattice solution of Anderson localization, Phys. Rev. B **109**, 174216 (2024).
[52] Y. Fyodorov, A. D. Mirlin, and H.-J. Sommers, A novel field theoretical approach to the Anderson localization: sparse random hopping model, J de Physique I **2**, 1571 (1992).
[53] A. D. Mirlin and Y. V. Fyodorov, Universality of level correlation function of sparse random matrices, J. Phys. A: Math. Gen. **24**, 2273 (1991).
[54] M. L. Mehta, *Random Matrices* (Elsevier, Amsterdam, 2004).
[55] A. P. Luca D'Alessio, Y. Kafri and M. Rigol, From quantum chaos and eigenstate thermalization to statistical mechanics and thermodynamics, Adv. Phys. **65**, 239 (2016).
[56] C. W. J. Beenakker, Random-matrix theory of quantum transport, Rev. Mod. Phys. **69**, 731 (1997).
[57] F. Evers and A. D. Mirlin, Anderson transitions, Rev. Mod. Phys. **80**, 1355 (2008).
[58] V. E. Kravtsov, I. M. Khaymovich, E. Cuevas, and M. Amini, A random matrix model with localization and ergodic transitions, New J. Phys. **17**, 122002 (2015).
[59] G. D. Tomasi, M. Amini, S. Bera, I. M. Khaymovich, and V. E. Kravtsov, Survival probability in generalized Rosenzweig-Porter random matrix ensemble, SciPost Phys. **6**, 014 (2019).
[60] G. Biroli and M. Tarzia, Lévy-Rosenzweig-Porter random matrix ensemble, Phys. Rev. B **103**, 104205 (2021).
[61] V. E. Kravtsov, I. M. Khaymovich, B. L. Altshuler, and L. B. Ioffe, Localization transition on the random regular graph as an unstable tricritical point in a log-normal Rosenzweig-Porter random matrix ensemble, arXiv:2002.02979.
[62] E. Bogomolny and M. Sieber, Eigenfunction distribution for the Rosenzweig-Porter model, Phys. Rev. E **98**, 032139 (2018).
[63] I. M. Khaymovich and V. E. Kravtsov, Dynamical phases in a "multifractal" Rosenzweig-Porter model, SciPost Phys. **11**, 045 (2021).
[64] I. M. Khaymovich, V. E. Kravtsov, B. L. Altshuler, and L. B. Ioffe, Fragile extended phases in the log-normal Rosenzweig-Porter model, Phys. Rev. Res. **2**, 043346 (2020).
[65] W. Buijsman and Y. B. Lev, Circular Rosenzweig-Porter random matrix ensemble, SciPost Phys. **12**, 082 (2022).
[66] P. von Soosten and S. Warzel, Non-ergodic delocalization in the Rosenzweig–Porter model, Lett. Math. Phys. **109**, 905 (2019).
[67] M. Sarkar, R. Ghosh, and I. M. Khaymovich, Tuning the phase diagram of a Rosenzweig-Porter model with fractal disorder, Phys. Rev. B **108**, L060203 (2023).
[68] W. Chen, O. Giraud, J. Gong, and G. Lemarié, companion paper, Describing the critical behavior of the Anderson transition in infinite dimension by random-matrix ensembles: Logarithmic multifractality and critical localization, Phys. Rev. B **110**, 014210 (2024).
[69] E. Abrahams, *50 years of Anderson Localization* (World scientific, University of California, Los Angeles, USA, 2010), Vol. 24.
[70] C. Castellani and L. Peliti, Multifractal wavefunction at the localisation threshold, J. Phys. A: Math. Gen. **19**, L429 (1986).
[71] A. Rodriguez, L. J. Vasquez, and R. A. Römer, Multifractal

analysis with the probability density function at the three-dimensional Anderson transition, Phys. Rev. Lett. **102**, 106406 (2009).
[72] S. Faez, A. Strybulevych, J. H. Page, A. Lagendijk, and B. A. van Tiggelen, Observation of multifractality in Anderson localization of ultrasound, Phys. Rev. Lett. **103**, 155703 (2009).
[73] A. Rodriguez, L. J. Vasquez, K. Slevin, and R. A. Römer, Multifractal finite-size scaling and universality at the Anderson transition, Phys. Rev. B **84**, 134209 (2011).
[74] G. Lemarié, J. Chabé, P. Szriftgiser, J. C. Garreau, B. Grémaud, and D. Delande, Observation of the Anderson metal-insulator transition with atomic matter waves: Theory and experiment, Phys. Rev. A **80**, 043626 (2009).
[75] G. Lemarié, H. Lignier, D. Delande, P. Szriftgiser, and J. C. Garreau, Critical state of the Anderson transition: Between a metal and an insulator, Phys. Rev. Lett. **105**, 090601 (2010).
[76] J. Chabé, G. Lemarié, B. Grémaud, D. Delande, P. Szriftgiser, and J. C. Garreau, Experimental observation of the Anderson metal-insulator transition with atomic matter waves, Phys. Rev. Lett. **101**, 255702 (2008).
[77] E. Cuevas, V. Gasparian, and M. Ortuño, Anomalously large critical regions in power-law random matrix ensembles, Phys. Rev. Lett. **87**, 056601 (2001).
[78] T. Ohtsuki and T. Kawarabayashi, Anomalous diffusion at the Anderson transitions, J. Phys. Soc. Jpn. **66**, 314 (1997).
[79] C. A. Müller, D. Delande, and B. Shapiro, Critical dynamics at the Anderson localization mobility edge, Phys. Rev. A **94**, 033615 (2016).
[80] R. Ketzmerick, G. Petschel, and T. Geisel, Slow decay of temporal correlations in quantum systems with Cantor spectra, Phys. Rev. Lett. **69**, 695 (1992).
[81] V. E. Kravtsov, A. Ossipov, O. M. Yevtushenko, and E. Cuevas, Dynamical scaling for critical states: Validity of Chalker's ansatz for strong fractality, Phys. Rev. B **82**, 161102(R) (2010).
[82] V. E. Kravtsov, A. Ossipov, and O. M. Yevtushenko, Return probability and scaling exponents in the critical random matrix ensemble, J. Phys. A: Math. Theor. **44**, 305003 (2011).
[83] B. Altshuler and V. Kravtsov, Random Cantor sets and mini-bands in local spectrum of quantum systems, Ann. Phys. **456**, 169300 (2023).
[84] S. Ghosh, C. Miniatura, N. Cherroret, and D. Delande, Coherent forward scattering as a signature of Anderson metal-insulator transitions, Phys. Rev. A **95**, 041602(R) (2017).
[85] M. Martinez, G. Lemarié, B. Georgeot, C. Miniatura, and O. Giraud, Coherent forward scattering as a robust probe of multifractality in critical disordered media, SciPost Phys. **14**, 057 (2023).
[86] P. Akridas-Morel, N. Cherroret, and D. Delande, Multifractality of the kicked rotor at the critical point of the Anderson transition, Phys. Rev. A **100**, 043612 (2019).
[87] W. Chen, G. Lemarié, and J. Gong, Critical dynamics of long-range quantum disordered systems, Phys. Rev. E **108**, 054127 (2023).
[88] B. B. Mandelbrot, Intermittent turbulence in self-similar cascades: divergence of high moments and dimension of the carrier, J. Fluid Mech. **62**, 331 (1974).
[89] B. B. Mandelbrot and B. B. Mandelbrot, *The Fractal Geometry of Nature* (WH freeman New York, 1982), Vol. 1.
[90] K. Falconer, *Fractal Geometry: Mathematical Foundations and Applications* (John Wiley & Sons, Hoboken, NJ, 2004).
[91] A. D. Mirlin, Y. V. Fyodorov, F.-M. Dittes, J. Quezada, and T. H. Seligman, Transition from localized to extended eigenstates in the ensemble of power-law random banded matrices, Phys. Rev. E **54**, 3221 (1996).
[92] A. D. Mirlin and F. Evers, Multifractality and critical fluctuations at the Anderson transition, Phys. Rev. B **62**, 7920 (2000).
[93] E. Bogomolny and M. Sieber, Power-law random banded matrices and ultrametric matrices: Eigenvector distribution in the intermediate regime, Phys. Rev. E **98**, 042116 (2018).
[94] E. Bogomolny, O. Giraud, and C. Schmit, Random matrix ensembles associated with lax matrices, Phys. Rev. Lett. **103**, 054103 (2009).
[95] E. Bogomolny and O. Giraud, Perturbation approach to multifractal dimensions for certain critical random-matrix ensembles, Phys. Rev. E **84**, 036212 (2011).
[96] E. Bogomolny and O. Giraud, Multifractal dimensions for all moments for certain critical random-matrix ensembles in the strong multifractality regime, Phys. Rev. E **85**, 046208 (2012).
[97] L. S. Levitov, Absence of localization of vibrational modes due to dipole-dipole interaction, Europhys. Lett. **9**, 83 (1989).
[98] L. S. Levitov, Delocalization of vibrational modes caused by electric dipole interaction, Phys. Rev. Lett. **64**, 547 (1990).
[99] C. Monthus and T. Garel, The Anderson localization transition with long-ranged hoppings: analysis of the strong multifractality regime in terms of weighted Lévy sums, J. Stat. Mech.: Theory Exp. (2010) P09015.
[100] E. Bogomolny and O. Giraud, Eigenfunction entropy and spectral compressibility for critical random matrix ensembles, Phys. Rev. Lett. **106**, 044101 (2011).
[101] O. Yevtushenko and A. Ossipov, A supersymmetry approach to almost diagonal random matrices, J. Phys. A: Math. Theor. **40**, 4691 (2007).
[102] A. D. Mirlin, Y. V. Fyodorov, A. Mildenberger, and F. Evers, Exact relations between multifractal exponents at the Anderson transition, Phys. Rev. Lett. **97**, 046803 (2006).
[103] I. A. Gruzberg, A. W. W. Ludwig, A. D. Mirlin, and M. R. Zirnbauer, Symmetries of multifractal spectra and field theories of Anderson localization, Phys. Rev. Lett. **107**, 086403 (2011).
[104] I. A. Gruzberg, A. D. Mirlin, and M. R. Zirnbauer, Classification and symmetry properties of scaling dimensions at Anderson transitions, Phys. Rev. B **87**, 125144 (2013).
[105] A. M. Bilen, B. Georgeot, O. Giraud, G. Lemarié, and I. García-Mata, Symmetry violation of quantum multifractality: Gaussian fluctuations versus algebraic localization, Phys. Rev. Res. **3**, L022023 (2021).
[106] A. Chen, J. Maciejko, and I. Boettcher, Anderson localization transition in disordered hyperbolic lattices, arXiv:2310.07978.
[107] A. M. García-García and J. Wang, Anderson transition in quantum chaos, Phys. Rev. Lett. **94**, 244102 (2005).
[108] B. V. Chirikov, A universal instability of many-dimensional oscillator systems, Phys. Rep. **52**, 263 (1979).
[109] F. M. Izrailev, Simple models of quantum chaos: Spectrum and eigenfunctions, Phys. Rep. **196**, 299 (1990).
[110] D. J. Luitz, Polynomial filter diagonalization of large Floquet unitary operators, SciPost Phys. **11**, 021 (2021).
[111] V. E. Kravtsov, O. M. Yevtushenko, P. Snajberk, and E. Cuevas, Lévy flights and multifractality in quantum critical

diffusion and in classical random walks on fractals, Phys. Rev. E **86**, 021136 (2012).

[112] R. Ketzmerick, K. Kruse, S. Kraut, and T. Geisel, What determines the spreading of a wave packet? Phys. Rev. Lett. **79**, 1959 (1997).

[113] J. Chalker, Scaling and eigenfunction correlations near a mobility edge, Physica A **167**, 253 (1990).

[114] J. Arenz and M. R. Zirnbauer, Wegner model on a tree graph: U(1) symmetry breaking and a non-standard phase of disordered electronic matter, arXiv:2305.00243.

[115] M. R. Zirnbauer, Wegner model in high dimension: U(1) symmetry breaking and a non-standard phase of disordered electronic matter, I. one-replica theory, arXiv:2309.17323.